Carbohydrate Polymers 89 (2012) 740–748

Contents lists available at SciVerse ScienceDirect

Carbohydrate Polymers

journal homepage: www.elsevier.com/locate/carbpol

Piroxicam loaded alginate beads obtained by prilling/microwave tandem technique: Morphology and drug release

Rita P. Aquino, Giulia Auriemma, Matteo d'Amore, Anna Maria D'Ursi, Teresa Mencherini, Pasquale Del Gaudio*

Department of Pharmaceutical and Biomedical Sciences, University of Salerno, I-84084 Fisciano (SA), Italy

ARTICLE INFO

Article history:
Received 19 January 2012
Received in revised form 28 March 2012
Accepted 2 April 2012
Available online 9 April 2012

Keywords:
Alginate beads
Prilling
Microwave treatments
Drug release
Drying rate
Piroxicam

ABSTRACT

This paper presents a tandem technique, based on the combination of prilling and microwave (MW) assisted treatments, to produce biodegradable alginate carriers of piroxicam with different drug controlled release behaviours. Results showed that alginate/piroxicam beads demonstrated high encapsulation efficiency and very narrow dimensional distribution. Beads dried by MW retained shape and size distribution of the hydrated particles while drying rate was strongly increased compared to convective drying processes. Moreover, different MW irradiation regimes promoted interactions between the drug and alginate matrix, affected drug polymorphism as well as inner and surface matrix structure leading to different piroxicam release profiles. High level MW irradiation led to beads with highly porous and swellable matrix able to release piroxicam in few minutes in the intestine while convective drying produced gastro-resistant beads that exhibit sustained piroxicam release (total release in 5.5 h) in intestinal environment. On these results the tandem technique prilling/MW irradiation appears to be promising to obtain alginate carrier with tailored NSAIDs release depending on drug characteristics and MW irradiation.

1. Introduction

Polysaccharides polymers such as alginates have been investigated in the last years as carrier for controlled drug release (Arica et al., 2005; Del Gaudio, Russo, Rosaria Lauro, Colombo, & Aquino, 2009), cell encapsulation (Tostões et al., 2011), tissue engineering material (Aguado, Mulyasasmita, Su, Lampe, & Heilshorn, 2011), or for taste masking in paediatric formulations (Chiappetta et al., 2009). The encapsulation property of alginate is due to its ability to move from sol to gel state by ionotropic gelation under mild conditions through interactions with bivalent or trivalent cations (Josef, Zilberman, & Bianco-Peled, 2010). The resulting particles are able to protect drugs from environmental stress or, based on alginate pH dependent solubility, from chemical/enzymatic digestion in gastric fluids (Gong et al., 2011). Moreover, mucoadhesive properties of the alginate may lead to an increase in residence time and reduction of drug metabolism (Elzatahry, Eldin, Soliman, & Hassan, 2009; Patil & Sawant, 2009). However, physical properties (mechanical strength, wettability, pore size and distribution) of particles are strongly influenced by both polymer characteristics and production technology as well as by curing/drying step (Del Gaudio, Colombo, Colombo, Russo, & Sonvico, 2005; Hegedus & Pintye-Hódi, 2007; Wong, Chan, Kho, & Sia Heng, 2002).

Alginate based beads are commonly manufactured by dropping drug–polymer solutions into a bivalent cations aqueous solution. Recently, prilling or laminar jet break-up has been applied for the beads production. This mild and easy scalable microencapsulation technique is based on the breaking apart of a laminar jet of polymer solution into a row of mono-sized drops by means of a vibrating nozzle device (Brandenberg & Widmer, 1998; Sakai, Sadataka, Saito, & Matsushita, 1985) that results in hydrated particles. Hydrated beads can be used as self-consistent dosage form or as building blocks in the production of controlled drug release platforms. However, beads need to be dried in order to stabilize the dosage forms and to avoid microbiological degradation. Thus, the drying process has a crucial role to assure the quality of the final product.

Among various drying technique, irradiation with microwaves (MW) has gained great interest in the last few years for its peculiar way of heating materials over conventional methods by interaction of the electromagnetic waves with the irradiated matter. MW has been mainly applied in the synthesis of organic compounds reducing time of reactions and solvent (Kappe & Dallinger, 2006; Lidström, Tierney, Wathey, & Westman, 2001), as much as in pharmaceutical formulation design as drying or curing process (McMinn, McLoughlin, & Magee, 2005) of solid dispersions,

* Corresponding author. Tel.: +39 089969247; fax: +39 089969602.
E-mail address: pdelgaudio@unisa.it (P. Del Gaudio).

0144-8617/$ – see front matter © 2012 Elsevier Ltd. All rights reserved.
http://dx.doi.org/10.1016/j.carbpol.2012.04.003

granules and tablets (Gainotti et al., 2006; Jamuna-Thevi, Zakaria, Othman, & Muhamad, 2009; Moneghini, Zingone, & De Zordi, 2009). The efficiency of MW-assisted drying process is strongly dependent both on the dielectric, thermal and other physical properties as well as on moisture content of the irradiated material. Therefore, beads with high water content are able to readily interact with microwaves for their dielectric constants that are the overriding factor affecting the efficiency of heat transfer and, in turn, drying performance (Hegedus & Pintye-Hódi, 2007; Loh, Liew, Lee, & Heng, 2008). Recently, we reported that the selective nature of MW irradiation, due to the permittivity (ε) of the alginate bead components, allows easy water elimination or moisture levelling in beads processed by prilling. In addition, different MW irradiation levels can modulate interactions between the dextran matrix and low melting point drugs such as ketoprofen, influencing the drug polymorphism, morphology and mechanical resistance of the beads as well as strongly affecting ketoprofen release behaviour (Auriemma, Del Gaudio, Barba, d'Amore, & Aquino, 2011).

Piroxicam is a well-known non-steroidal anti-inflammatory drug (NSAID) exhibiting analgesic and antipiretic properties and used in the management of chronic diseases. Although, it is included in the class II of the Biopharmaceutical Classification System (BCS) as ketoprofen, this oxicam derivative possess different physical–chemical properties such as higher melting point and ampholite nature and may exist in different ionic forms at physiological pH (Geckle, Rescek, & Whipple, 1989). As other NSAIDs, piroxicam has severe side-effects, mainly gastric lesions or ulcers. Therefore, there is a considerable interest in developing new enteric formulations, poorly adsorbed through the gastric mucosa but able to swell and release in the intestinal lumen, which may exerts less gastric direct acute damage bypassing the stomach (Debunne, Vervaet, Mangelings, & Remon, 2004; Obeidat & Price, 2006). In addition, a prolonged intestinal residence time could be useful for the treatment of severe chronic mucosal inflammations such as inflammatory bowel diseases (IBD).

In the present work we investigated the feasibility of the application of a tandem technique based on prilling and MW irradiation in producing alginate/piroxicam beads able to control drug release in the gastro-intestinal tract. With this aim we produced beads by prilling in different drug/polymer ratios, and they were successively dried at four different MW irradiation levels (I–IV). The effect of process variables on drying kinetics and particle properties (surface and inner characteristics, drug–polymer interactions, drug polymorphism) were studied. Finally, the release behaviour of piroxicam by comparison to those beads dehydrated by conventional convective methods (room conditions and tray oven) was also investigated (using a pH-change method).

2. Materials and methods

2.1. Materials

Sodium alginate European Pharmacopoeia X (MW ≈ 240 KDa, β-D-mannuronic:-l-guluronic acid ratio of 1.2) (Carlo Erba, Milan, I) employed as matrix in the preparation of gel-beads was used as purchased, without further purification. Water content (5%, w/w) was determined by Karl Fischer titration (Tritomatic KF, Crison Instruments, SA, Barcellona, SP). $CaCl_2$ anhydrous, granular (Sigma–Aldrich, Milan, I) was used in aqueous solution as cross-linking agent.

Piroxicam was kindly donated by Sifavitor (Sifavitor srl, Milan, I).

All other chemicals and reagents were obtained from Sigma Aldrich (Milan, I) and used as supplied.

2.2. Drug loaded hydrated beads preparation

An appropriate amount of sodium alginate was dissolved in distilled water at room temperature under gentle stirring for 18 h in order to obtain 100 ml of polymer solution with concentrations ranging between 1.50% and 2.00% (w/w). Different amounts of solid piroxicam (mean diameter 31.06 μm, span 28.36 μm) were suspended into the polymer solution and stirred for 2 h in order to obtain different drug/polymer ratios (between 0.10 and 0.33). Beads were manufactured by a vibrating nozzle device (Nisco Encapsulator Unit, Var D; Nisco Engineering Inc., Zurich, CH), equipped with a syringe pump (Model 200 Series, Kd Scientific Inc., Boston, MA, USA), pumping the drug/polymer solution through a nozzle 400 μm in diameter. Experiments were performed at various volumetric flow rates, between 10 and 18 ml/min. Vibration frequency used to break up the laminar liquid jet was set between 250 and 300 Hz, amplitude of vibration 100%. The distance between the vibrating nozzle and the gelling bath was fixed at 25 cm. A stroboscopic lamp was set at the same amplitude as the frequency, in order to visualize the falling droplets. These latter were collected into an aqueous solution 0.3 M $CaCl_2$ where they were gelified under gentle stirring. The beads were held into the gelling solution for 10 min at room temperature then recovered and thoroughly rinsed with distilled water.

2.3. Beads drying

A commercial multimode microwaves cavity (MW480 7-Days, De Longhi, Treviso, I) was used as MW drying apparatus. The MW source had a nominal power of 700 W (continuous regime) and a built-in duty cycle to simulate different power levels of 490 W, 350 W, 245 W (discontinuous regime) achieved through on/off cycles. They are hereafter reported as levels IV–I, respectively. The irradiation time was set using an integrated timer. Desired power and irradiation time were selected using a touch-control panel. The MW oven was equipped with a rotating pyrex plate and an appropriate sample-support to let uniform irradiation of the beads.

In brief, weighed amount of beads (about 2 g) was subjected to microwave treatments at various combinations of irradiation in time. The weight variation of beads was determined before and after the beads irradiation by using a four decimal place electronic balance (Crystal 200 CAL, Gibertini, Milan, I).

Residual moisture content, assayed by gravimetric method, was expressed as the moisture ratio, MR, i.e. ratio between actual and initial moisture.

Beads were also dried by convective conventional methods using a tray oven (ISCO mod. 9000, Milan, I) at 105 °C and using room conditions (22 °C; 67% RH). All the drying runs were stopped when a constant weight was achieved (moisture ratio was evaluated as previously reported). Beads dried by convective methods were used as control.

2.4. Beads size and morphology

Size distribution of hydrated and dried beads were measured by both an optical microscope (Citoval 2, Alessandrini, Milan, I) equipped with a camera and laser light scattering spectroscopy (Coulter LS 13320, Beckman Coulter, Inc., Brea, CA, USA) equipped with a 12 ml micro liquid module. The LS 13320 uses a 5 mW laser diode with a wavelength of 750 nm, reverse Fourier optics and binocular lens systems. During preliminary studies, ethanol was chosen as suspending medium. Beads were suspended into the small-volume cell filled with ethanol to obtain an obscuration between 10% and 12%. The particle size distribution was calculated by the instrument software, using the Fraunhofer model. The analyses were carried out in triplicate for each sample.

Scanning electron microscopy (SEM) was performed using a Carl Zeiss EVO MA 10 microscope with a secondary electron detector (Carl Zeiss SMT Ltd., Cambridge, UK) equipped with a LEICA EMSCD005 metallizator producing a deposition of a 200–400 Å thick gold layer. Analysis was conducted at 20 keV.

Projection diameter was obtained by image analysis (Image J software, Wayne Rasband, National Institute of Health, Bethesda, MD, USA). A minimum of one hundred bead images were analyzed for each preparation in order to calculate length-number mean and relative standard deviation for at least three different prilling processes. Perimeter and projection surface area obtained by image analysis were used to calculate a sphericity coefficient (SC) by the following equation (Almeida-Prieto, Blanco-Méndez, & Otero-Espinar, 2004, 2006):

$$SC = \frac{4\pi A}{P^2}$$

where A is the projected bead surface area and P its perimeter.

Surface roughness (SR) was calculated using fractal descriptors obtained by grey level distribution analysis measured on the SEM images of the beads. The images were taken at the same magnification. A scanned area of the SEM image, a box of 200 μm width and 200 μm length, was analyzed by Image J software using the algorithm known as the "box counting method" (Chappard et al., 2003). The analysis was carried out on 5 different area sections for each bead image considered and a mean fractal descriptor was obtained. The analysis was repeated on at least 10 beads for each batch.

2.5. Swelling kinetics of dried beads

Swelling experiments were performed in a USP 27 dissolution apparatus II: paddle, 100 rpm, 37 °C (Sotax AT7 Smart – Sotax, CH) using simulated gastric fluid (SGF), simulated intestinal fluid (SIF) (USP 27). In order to evaluate the swelling profiles, dried beads were placed in a vessel containing 1 l of buffer under stirring, then, using an optical microscope equipped with a video camera, the bead volume was measured in swollen state at different times and compared with the volume in dry state. The degree of swelling, or swelling ratio, was calculated as the ratio between the bead volume in swollen and dry states.

2.6. Calorimetric analysis

Beads thermal characteristics were determined by differential scanning calorimetry (DSC) (Mettler Toledo DSC 822e module controlled by Mettler Star E software, Columbus, OH, USA), and compared with those obtained using both blank beads and drug as raw material. An appropriate amount of dried beads was crimped in a standard aluminium pan that was pierced and heated from 25 to 350 °C at a scanning rate of 10 °C/min. Characteristic peaks were recorded and specific heat of the melting endotherm was evaluated. At least duplicates were carried out for each batch of sample, and the results averaged.

Thermo gravimetric analysis (TGA) was carried out in order to evaluate the water content in the different batches of dried beads (TG50 – Mettler Toledo, USA). Analyses were conducted at 10 °C/min heating rate in the range 25–200 °C.

Both DSC and TGA were performed in nitrogen atmosphere at a flow rate of 100 ml/min.

2.7. FTIR analysis

FTIR analysis was performed in a FTIR spectrophotometer (FT-IR Nexus, Thermo-Nicolet, West Palm Beach, FL, USA) equipped with a mercury–cadmium–telluride detector. The samples (piroxicam, blank and piroxicam loaded beads) were combined with small amount of potassium bromide and pressed to 3 tonnes in a manual press (OMCN s.p.a., Bergamo, I). The thin compacts produced were analyzed using 256 scans with a 1 cm^{-1} resolution step. Each experiment was carried out in triplicate, and results averaged.

2.8. Powder X-ray diffraction studies (XRPD)

Dried samples were studied by means of X-ray diffraction measurement (XRD) with a Rigaku D/MAX-2000 diffractometer (Rigaku Corporation, Tokyo, J) using a Ni-filtered Cu Kα radiation (40 kV, 20 A). 2θ range was set from 5° to 50°, step size 0.03°/2θ and 5 s counting time per step. A Rigaku imaging plate, mod. R-AXIX DSBC, was used for digitizing the diffraction patterns.

2.9. Drug content and encapsulation efficiency

Accurately weighed amounts of beads from each manufactured batch (about 50 mg each) were dissolved under vigorous stirring in PBS buffer (100 mM). Piroxicam content was determined by UV spectroscopy at λ 354 nm (Lambda 25 UV/VIS Spectrometer, PerkinElmer, Waltham, MA, USA). Encapsulation efficiency was calculated as the ratio of actual to theoretical drug content. Each analysis was performed in triplicate; results were expressed in terms of mean ± standard deviation. Both drug content and encapsulation efficiency were calculated correcting the weight for the residual water and calcium chloride contained into the beads, as previously determined by Karl Fischer titration (Tritomatic KF, Crison Instruments, SA, Barcellona, SP) and EDTA titration, respectively.

2.10. Kinetics of drug release

In vitro dissolution/release tests were conducted in sink conditions on given amounts of beads containing about 20 mg of drug using a USP 27 dissolution apparatus II: paddle, 100 rpm, 37 °C (Sotax AT7 Smart – Sotax, Allschwil, CH) on line with a UV spectrophotometer (Lambda 25 UV/VIS Spectrometer, Perkin Elmer, Waltham, MA, USA). Briefly, dried beads were added to the dissolution medium, 750 ml 0.1 M HCl for 2 h, then 250 ml of 0.20 M Na_3PO_4 was added and pH adjusted to 6.8 as described in the USP 27/NF monograph "Drug release from delayed-release articles". Data were analyzed spectrophotometrically at λ 333 and 354 nm, for gastric and intestinal simulated environment, respectively. Dissolution tests were conducted on six different batches of particles; mean values and standard deviation were evaluated.

3. Results and discussion

3.1. Production and preliminary characterization of hydrated and dried beads

Alginate/piroxicam beads were produced by a Nisco Encapsulator VarD unit equipped with a nozzle of 400 μm diameter using feed at alginate concentrations ranging between 1.50% and 2.00% (w/w). As previously described, other process variables as volumetric flow rate, nozzle vibration frequency and amplitude were set according to the cross model in order to achieve beads diameter distribution as narrow as possible (Auriemma et al., 2011; Del Gaudio et al., 2009; Soong & Shen, 1981). Results from size and morphology analyses showed that the selected conditions enable the production of spherical hydrated beads. Typically, piroxicam hydrated beads had an average mean size ranging between 2052 and 2086 μm (relative standard deviation lower than 3%, see Table 1) and a sphericity coefficient (SC) of 0.98 ± 0.02 (where 1 corresponds to a sphere), with a smooth and regular surface. Micrometric spots corresponding to

Table 1
Feed solution and mean diameter in both hydrated and dried state of beads manufactured by prilling. Each value represents the mean diameter ± S.D. ($n = 3$).

Alginate solution (%, w/w)	Piroxicam polymer ratio	Hydrated beads (μm)	Air-dried (μm)	Oven dried (μm)	MW level IV (μm)	MW level III (μm)	MW level II (μm)	MW level I (μm)
1.50	1:10	2052 ± 42	1212 ± 29	1226 ± 31	1228 ± 32	1226 ± 37	1225 ± 36	1222 ± 33
	1:3	2067 ± 35	1235 ± 27	1238 ± 37	1231 ± 34	1232 ± 29	1239 ± 38	1229 ± 33
1.75	1:10	2058 ± 32	1223 ± 29	1228 ± 30	1219 ± 35	1246 ± 38	1228 ± 32	1236 ± 36
	1:3	2074 ± 39	1244 ± 32	1218 ± 31	1232 ± 31	1239 ± 29	1235 ± 34	1222 ± 34
2.00	1:10	2079 ± 34	1216 ± 35	1229 ± 24	1235 ± 40	1231 ± 36	1236 ± 32	1219 ± 29
	1:3	2086 ± 31	1222 ± 34	1232 ± 28	1230 ± 31	1229 ± 29	1219 ± 33	1222 ± 38

Air-dried: beads dried at room conditions.
Oven dried: beads dried at 105 °C.
MW: beads dried by microwave exposure at different irradiation level.

solid piroxicam were recognizable inside the bead light structure by optical microscopy analysis (data not shown).

The drying process was conducted using homogenous amounts of hydrated beads exposed to air at room conditions, air-bulk heating (tray oven) at 105 °C and microwave assisted heating at different regimes of irradiation (MW, power levels IV–I, where level IV corresponds to continuous irradiation and levels III–I to discontinuous irradiation at decreasing nominal power).

Remarkably high values of encapsulation efficiency (over 85% for each batch) were obtained; drug content increased from 7% to 25% in accordance with the increasing of drug/alginate ratio (0.10–0.33), regardless of the drying process used.

3.2. Influence of drying processes on beads drying kinetics

Drying rates were affected by the different energy transfer mechanism assisted by microwaves or convective heating. Typically, conventional convective drying methods required longer heating times due to the low thermal diffusivity of hydrated beads. Indeed, 7 h were necessary to dry beads by tray oven process, while beads exposed at room conditions required 12–18 h depending on alginate solution concentration (Fig. 1). Fig. 1 also shows that the drying rate was found to be faster for dielectric heating and that the beads constant weight was achieved with shorter processing times. However, different MW regimes of irradiation affected drying profiles. In fact, MW irradiation at higher levels (levels IV–III) required 20–60 min to produce dried beads, while 120 and 180 min were required for levels II and I, respectively. As previously observed for beads loaded with ketoprofen, MW treatments at the discontinuous level III and at the continuous irradiation level IV produced similar drying rate only at the beginning of the process when water content of both beads was very high and the internal thermal gradient should have the same value. An easier diffusion of moisture

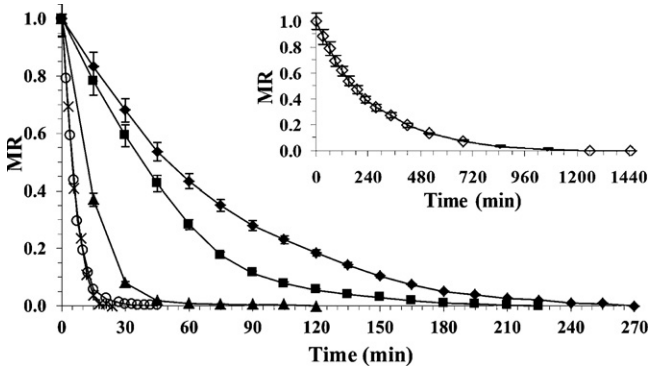

Fig. 1. Drying curves of 7% (w/w) piroxicam loaded beads produced with 1.75% (w/w) alginate solution dried at different microwave irradiation levels: IV (-*-); III (-○-); II (-▲-); I (-■-); tray oven drying at 105 °C (-◆-) and room conditions drying (-◇-) are also reported. Mean ± S.D ($n = 6$).

and vapour inside the polymer matrix layers occurs as well as a very fast elimination of water from beads when MW irradiation was switched off for short period of time (Araszkiewicz, Koziola, Lupinskaa, & Lupinskia, 2006), such as in MW level III. As drying process goes on different drying rates were observed because of the reduction of the thermal gradient and the decrease of water content inside the beads.

According to previous studies on dextran/ketoprofen particles (Del Gaudio et al., 2009; Hegedus & Pintye-Hódi, 2007), drying kinetics of alginate/piroxicam beads resulted strictly dependent on the drying process applied and independent on both drug loading and polymer solution concentration. Only beads produced with the highest alginate concentration (2.00%, w/w) and dried at lower level of irradiation required an overtime of 25 min more to achieve a zero moisture residue.

3.3. Influence of drying processes on beads micromeritics and piroxicam solid state

Mean diameter of beads dried at different conditions reduced to about 1200 μm (relative standard deviation lower than 3%) because of the shrinking of volume due to the loss of water. Not significant difference in volume shrinkage and dimensional distribution ($p < 0.005$) was recognized by optical microscopy and laser light scattering (LLS) in any batch produced (Table 1); differently, shape and surface roughness were dependent on both alginate concentration and drying process applied. As an example, SEM images of 1.75% (w/w) alginate beads loaded with 7% (w/w) piroxicam are reported in Figs. 2 and 3. We observed that sphericity coefficient (SC) was significantly reduced from 0.98 ± 0.02 for hydrated beads to 0.92 ± 0.06 and 0.91 ± 0.07 for beads dried by both convective methods, as shown in Fig. 2a. The largest differences in SC for beads dried by MW were found when alginate concentration at 2.00% (w/w) was used, with values decreasing of about 3% on hydrated beads.

In addition, convective dried beads exhibited a very rough surface (Fig. 3a). The surface roughness (SR) decreased from 1.82 ± 0.05 to a minimum of 1.74 ± 0.06 as the sodium alginate concentration increased. Interestingly, both convective drying methods produced beads with intact primary physical structure and few small cracks on their surface because of the slower and gentler elimination of moisture from the polymer matrix. By contrast, MW drying, as a result of the sudden temperature change owing the rapid expulsion of moisture, promoted the formation of irregular and porous structures with a large network of cracks which can considerably affect beads properties. The extension of the cracks and craters network increased when higher MW regimes of irradiation were applied (Fig. 2b and c). This phenomenon was particularly evident for beads dried at level IV (Fig. 2c and d) likely due to the higher temperature produced inside the beads that may result in the collapsing of the Ca^{2+} cross-linked alginate matrix (Figs. 2d and 3b, c) (Araszkiewicz

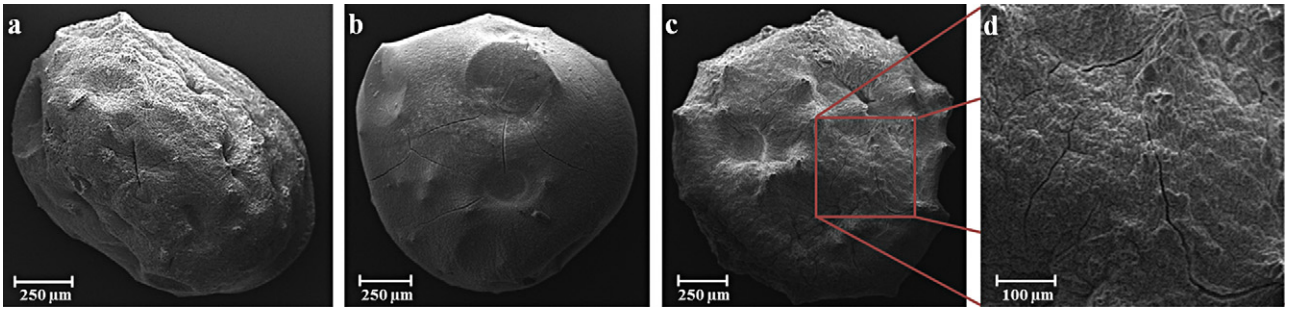

Fig. 2. SEM microphotographs of beads produced with 1.75% (w/w) alginate solution and loaded with 7% (w/w) piroxicam dried in different conditions: at room conditions (a), level I MW irradiation (b), level IV MW irradiation at different magnifications (c) and (d), respectively.

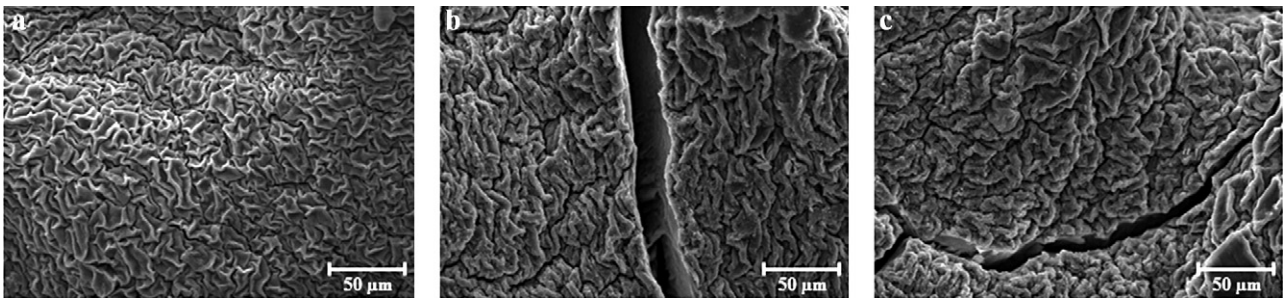

Fig. 3. SEM microphotographs of the surface of beads produced with 1.75% (w/w) alginate solution and loaded with 7% (w/w) piroxicam dried by air at room conditions (a), level I and level IV microwave irradiation (b and c).

et al., 2006). Otherwise, particle mean diameter ranging between 1195 ± 22 μm and 1184 ± 18 μm and surface roughness ranging between 1.68 ± 0.07 and 1.62 ± 0.04, were not very different in beads MW dried both at continuous regime or level I (Table 1 and Fig. 3).

In addition SEM analyses at higher magnification demonstrated that MW drying process affected the solid state of piroxicam entrapped within the Ca^{2+} crosslinked alginate matrix. In fact, beads with small spots of crystalline piroxicam were observed coming out of the surface in beads dried by MW at levels III–IV (Fig. 4b and c) whereas unspotted surface (Fig. 4a) were obtained by both level I MW irradiation and convective heating. As reported in the literature, amorphous piroxicam shows a strong tendency to crystallize in either cubic (β) or needle form (α) (Vrecer, Vrbinc, & Meden, 2003). When irradiation was conducted at MW level IV (Fig. 4c), exclusively the cubic form of crystalline piroxicam was recognized. Interestingly, both polymorphs (β cubic and α needle forms) were observed when MW level III was applied (Fig. 4b), probably due to by the high thermal gradient produced at the beginning of the drying and a different cooling phase at the end of the process. The amount of piroxicam in needle form was higher when higher drug/polymer ratio was used.

3.4. FT-IR, thermal analysis and XRPD of the beads

FT-IR, DSC and XRPD analyses gave further information on the solid state of piroxicam and the rearrangement of the alginate matrix.

As shown in Fig. 5d, piroxicam as crystalline raw material showed IR peaks at 3338 cm^{-1} relative to stretching of H-bonded NH, at 1638 cm^{-1} due to the stretching of carbonyl of the amide group, at 1602 cm^{-1} for the OH bending due to the amide group, and at 1530 cm^{-1} that refers to the stretching of C=N.

The FT-IR spectrum of Ca^{2+} crosslinked alginate beads, blank and dried at room conditions (Fig. 5a), is characteristic of a Ca^{2+}/alginate complex (Wong et al., 2002), the band at 1625 cm^{-1} and 1435 cm^{-1} corresponding, respectively, to the stretching of symmetric and asymmetric carboxylic groups of the dextrane, taking part in the coordination between the metal ion and the functional groups of the polymer. The shift of these peaks observed in MW dried beads (Fig. 5b and c) was directly correlated to the MW intensity suggesting an increase of the bond strength between Ca^{2+} and alginate, as previously observed (Auriemma et al., 2011).

The FT-IR spectra of MW dried and loaded beads (Fig. 5f and g) showed the disappearance of the peak at 3338 cm^{-1} and differences

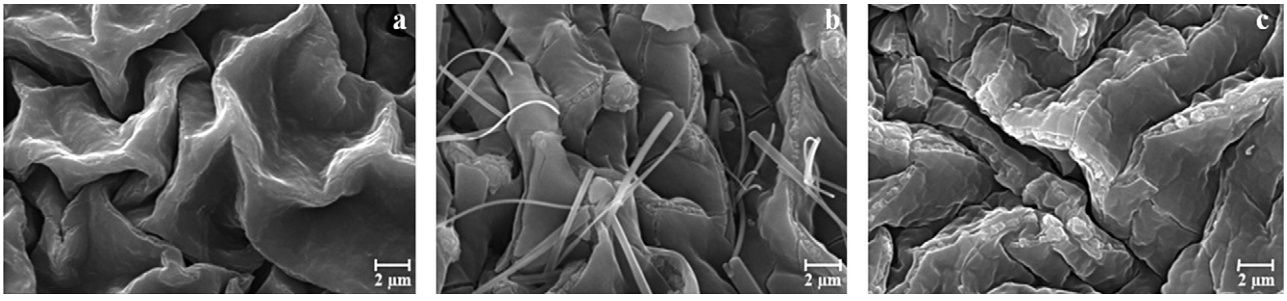

Fig. 4. SEM microphotographs of the surface of beads produced with 1.75% (w/w) alginate solution and loaded with 7% (w/w) piroxicam after microwave irradiation at level I with unspotted surface (a) and MW treatment at different irradiation levels: III and IV (b and c with crystalline piroxicam).

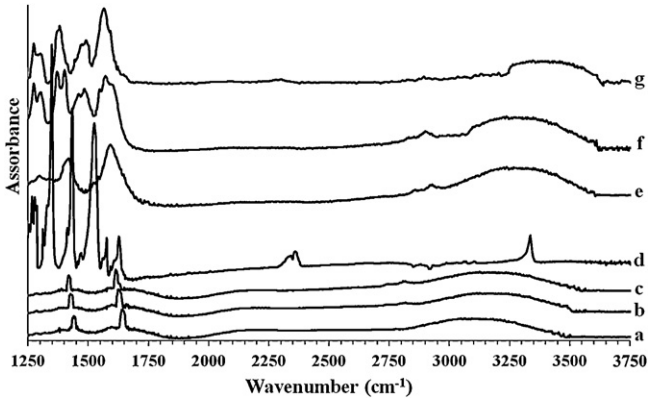

Fig. 5. FTIR spectra of piroxicam, 1.75% (w/w) blank alginate beads and 7% (w/w) drug loaded correspondent beads: blank alginate beads dried at room conditions (a), blank microwave dried beads at level I (b) and level IV (c), piroxicam (d), piroxicam loaded beads dried at room conditions (e); piroxicam loaded beads dried by microwave at level I (f) and at level IV (g).

in the C=N stretching region where piroxicam bands between 1640 and 1530 cm^{-1} were shifted to lower wavenumbers and merged in a broader peaks. Moreover, the peaks relative to carboxyl groups of the polymeric chain were lost. The observed signal shifting or loss suggests the occurrence of new interactions between piroxicam and polymer matrix which intensity were directly correlated with irradiation time exposure. This hypothesis is supported by the lowering in O–H absorption band intensity (about 3350 cm^{-1}) of polymer that is indicative of a decrease in alginate intramolecular bonding via Ca^{2+} (Li et al., 2009; Tam et al., 2005).

As reported in the literature and shown in its DSC thermogram (Fig. 6d), raw crystalline piroxicam is characterized by a melting endothermic peak at 202 °C and a large exothermic peak at 252 °C due to oxidative degradation (Vrecer et al., 2003). Ca^{2+}-crosslinked alginate beads, blank and dried by convective methods, exhibited a broad endothermic signal at 95 °C corresponding to water loss, and a peak at 182 °C due to melting process of the alginate complex with Ca^{2+} (Fig. 6a). MW treatment, depending on the irradiation time, shifted the last peak to higher temperature (185–202 °C) (Fig. 6b and c). This behaviour may depend upon the strength of the chelation between Ca^{2+} and alginate. In addition, DSC analysis did not give any evidence of piroxicam melting for beads MW dried at levels I and II (Fig. 6f) while a small peak at 202 °C, included in the melting peak of the alginate/Ca^{2+} complex, was observed in the thermograms of beads MW dried at levels III and IV (Fig. 6g). This observation was in agreement with XRPD and SEM analyses that indicated the presence of residual drug crystals on beads surface.

Finally, X-ray powder diffraction patterns in Fig. 7 confirmed the presence of crystalline piroxicam in the β cubic form on beads dried by MW at level IV (Fig. 7b) and in both polymorphic (β and α) forms on beads dried by MW at level III (Fig. 7c) with peaks around 13, 18 and 33 of 2-theta degrees typical of piroxicam in the α_1 form (Fortunato de Carvalho Rocha, Sabin, Março, & Poppi, 2011; Vrecer et al., 2003). Moreover, Fig. 7d and e did not show any crystalline diffraction pattern of piroxicam, confirming that solid drug was absent on the surface of beads dried by both MW at level I and by convective methods.

3.5. Influence of drying processes on piroxicam release behaviour

Release profiles of pure piroxicam and 7% (w/w) drug loaded beads produced with 1.75% (w/w) alginate solution obtained by different drying methods are shown in Fig. 8, as examples.

Owing to the pH dependent solubility of Ca^{2+}-alginate matrix, dissolution profile of piroxicam from beads dried at room conditions were typical of gastroresistant oral dosage forms releasing less than 20% of piroxicam in simulated gastric fluid (SGF – pH 1.2), one of the most important USP requirements for enteric formulations. The complete encapsulation of the drug into an intact and close alginate matrix may explain this behaviour. Nevertheless an interesting prolonged residence time was obtained in SIF at any polymer concentration; beads achieved complete piroxicam liberation from polymer matrix in simulated intestinal fluid (SIF – pH 6.8) in about 5 h, following the disintegration/swelling mechanism

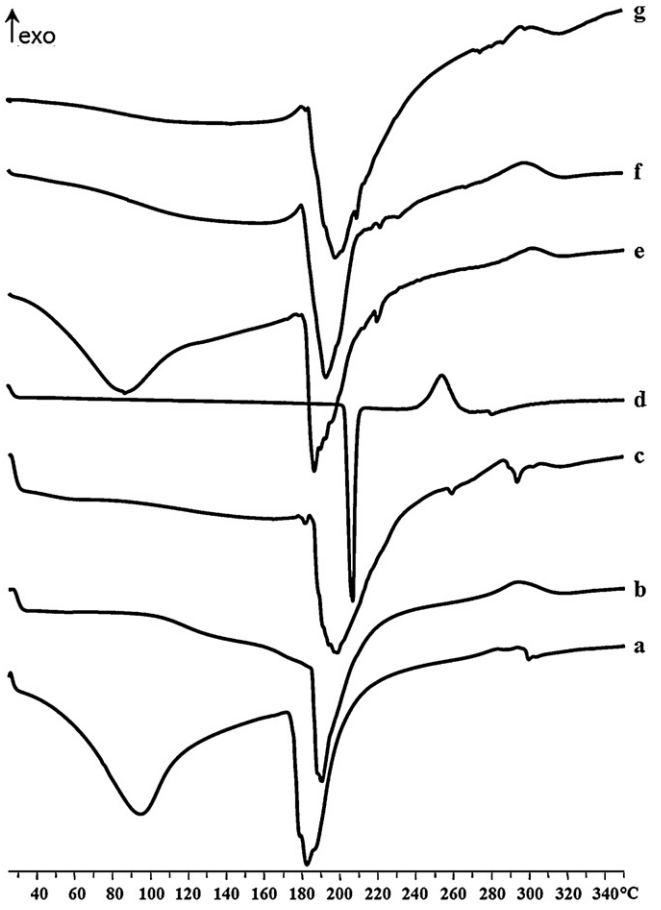

Fig. 6. Differential scanning calorimetry thermographs of blank alginate beads produced with 1.75% (w/w) alginate solution and dried at room conditions (a), MW irradiation at level I (b), level IV (c), pure piroxicam (d) and 7% (w/w) piroxicam loaded beads dried at room conditions (e) and by microwave irradiation at level I (f) and level IV (g).

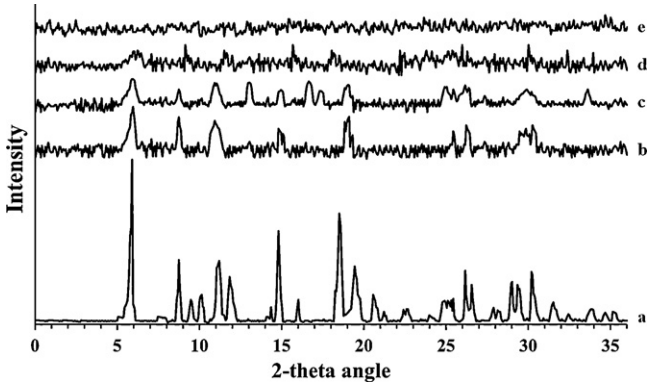

Fig. 7. X-ray diffraction patterns of raw crystalline piroxicam (β form) (a); 25% (w/w) piroxicam loaded alginate beads treated at different microwave power levels: IV (b), III (c), level I (d) and dried at room conditions (e).

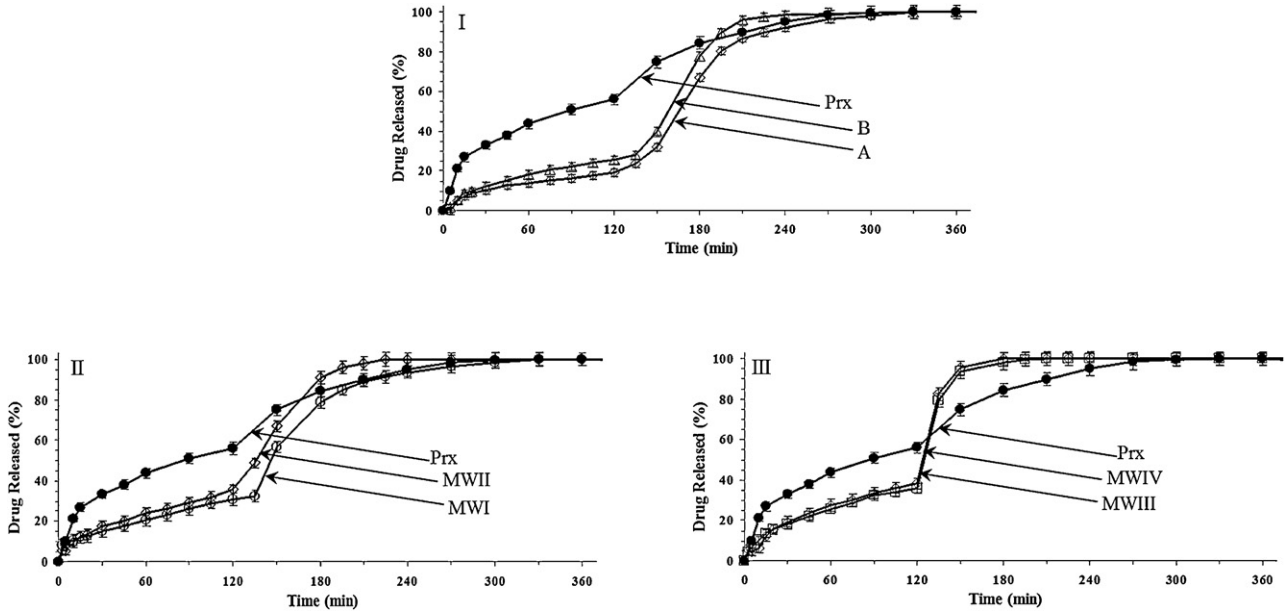

Fig. 8. Release profiles of pure piroxicam (Prx) and dried beads formulated with 1.75% (w/w) alginate solution and loaded with piroxicam 7% (w/w) dried by: exposition at room temperature (A), tray oven at 105 °C (B) and microwave treatments at: level I (MWI), level II (MWII), level III (MWIII) and level IV (MWIV). Mean + S.D ($n = 6$).

of the Ca^{2+} alginate matrix. On the contrary, 58% of the total amount of commercially available pure piroxicam dissolved in SGF whereas total dissolution was obtained after 3.5 h in SIF (Fig. 8I).

Piroxicam loaded in oven dried beads dissolved in SGF between 21% and 31% depending on polymer concentration and drug total liberation was achieved in SIF in about 3 h. The observed increase in release rate in SGF may be due to a fraction of piroxicam beneath the surface, as a consequence of convective drying at higher temperature (Hegedus & Pintye-Hódi, 2007) (105 °C). The internal moisture transfer to the beads surface and subsequent evaporation may drive the drug migration process.

Differently, any level of MW irradiation improved dissolution of piroxicam producing faster release kinetics. The amount of piroxicam released in SGF from all MW dried beads was in the range 30–38%. In the case of MW I and II dried beads, see Fig. 8II, drug release was prolonged till 120 min in SIF whereas beads MW dried at levels III and IV allowed total liberation of piroxicam in 50 min after the change of pH, with an high increase of dissolution rate compared to pure piroxicam, as shown in Fig. 8III.

Unlike alginate/ketoprofen beads, where the drug in amorphous or crystalline state on the beads surface affected release rate (Auriemma et al., 2011), release of piroxicam is not influenced by cubic or needle crystalline forms. By contrast, results suggest that surface and inner characteristics of the alginate/piroxicam beads (roughness, network of cracks and a fraction of crystalline piroxicam on beads surface) are strongly able to modulate the drug dissolution. In order to verify the effect of MW treatment on beads swelling properties, subsequent pore size increase and diffusion of the drug out the matrix, a series of swelling assay were performed for all samples.

Results demonstrated that alginate/piroxicam beads when dried by both convective methods exhibited low swelling properties as indicated by their SwR (swelling ratio). Convective dried beads reached SwR around 3.0 in SGF in about 90 min then retained the same volume as long as pH remained constant at 1.2, and SwR around 3.5 in SIF after 120 min (Fig. 9). Subsequently, it is suggested that the bead structure was slowly disaggregated and dissolution of piroxicam from the swollen beads was delayed, following the mechanism of capturing of the calcium ions by phosphate ions contained in SIF buffer (Bajpai & Sharma, 2004; Del Gaudio et al., 2005). MW level I treated beads showed slightly higher values of SwR reached both in SGF (3.5) and SIF (5.3–6 depending on alginate concentration) in 120 min according to the dissolution results. Very different swelling profiles were obtained for MW levels IV–III treated beads. SwR increased to its maximum, about 10, in 150 min (see Fig. 9) then swollen beads rapidly disaggregated, explaining piroxicam fast release in SIF observed in the dissolution tests. Moreover, it is interesting to point out that both formulations were able to float after 90 min in simulated gastric fluid and still floated till maximum swelling was reached. As regards this phenomenon, it could be justified by the entrapment of air into the inner highly porous structure of the beads while the outer layers started to swell (Kowalczuk, Sahbaz, & Drzymala, 2011; Streubel, Siepmann, & Bodmeier, 2002). The observed critical swelling and floating properties of beads dried by MW seem to be the controlling factor in release behaviour and may explain the observed increase in piroxicam release rate with respect to beads dried by convective techniques.

Polymer concentration did not influence significantly release profiles for MW IV–III dried beads whereas for MW I–II treated beads was observed a reduction in release rate of about 8%, comparing, as an example, 2.00% (w/w) alginate manufactured beads with respect to 1.50% (w/w), as shown in Fig. 10. On the contrary,

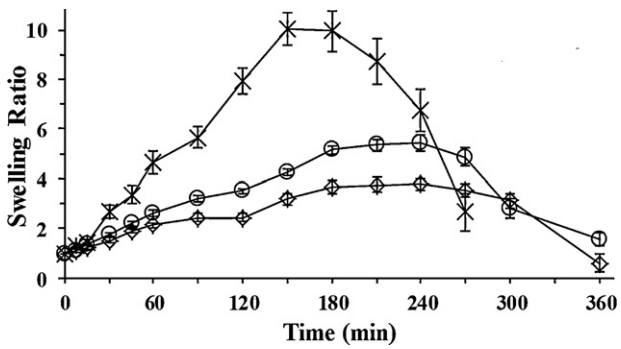

Fig. 9. Swelling profiles of 7% (w/w) piroxicam loaded beads produced with 1.75% (w/w) alginate solution dried by exposure to air (–◊–) and MW treatment at level I (–○–) and level IV (–*–). Mean ± S.D ($n = 6$).

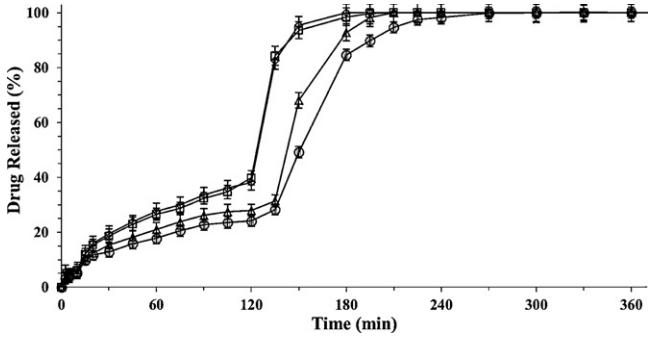

Fig. 10. Release profiles of beads loaded with 7% (w/w) piroxicam formulated with different alginate solutions and dried by microwave irradiation at level I: (–○–) 2.00% (w/w) and (–△–) 1.50% (w/w) alginate solution; level IV microwave irradiation: (–□–) 2.00% (w/w) and (–◇–) 150% (w/w) alginate solution. Mean ± S.D (n = 6).

drug loading had no impact at all on piroxicam release profiles or rate on any MW dried beads (data not shown).

4. Conclusions

This study showed that prilling technique in combination with MW drying process can be used as a simple tandem encapsulation/curing method to formulate alginate/piroxicam particles in very narrow size distribution. In particular, microwave treatment is an interesting alternative to the convective drying methods in the case of a high melting point and ampholite drugs, as piroxicam. MW treatment did not influence drug content and, accordingly, encapsulation efficiency (over 83%) while reduced drying time and allowed to control drying kinetics. Moreover, the use of MW at different irradiating regimes is able to modulate piroxicam release from alginate matrix affecting matrix structure and, consequently, swelling property, as critical factor controlling piroxicam release behaviour.

On these results the tandem technique based on prilling and MW treatments appears to be promising to obtain alginate carrier systems with tailored drug release profiles. Indeed, compared to conventional drying techniques, MW irradiation offers several advantages such as faster drying kinetics and reduced process times leading to lower operating costs.

Acknowledgements

The authors would like to thank MIUR (Ministero dell'Istruzione, dell'Università e della Ricerca) for financial support within PRIN project "Design and development of microsystems (gel-beads) for drug delivery by laminar jet break-up and dielectric treatments".

This work has been done as part of the research project "Progettazione e Sviluppo di Sistemi Terapeutici per il Rilascio Controllato di Famaci Attivi nelle Early Morning Pathologies" within POLIFARMA PON program.

References

Aguado, B., Mulyasasmita, W., Su, J., Lampe, K. J., & Heilshorn, S. (2011). Improving viability of stem cells during syringe needle flow through the design of hydrogel cell carriers. *Tissue Engineering Part A*.

Almeida-Prieto, S., Blanco-Méndez, J., & Otero-Espinar, F. J. (2004). Image analysis of the shape of granulated powder grains. *Journal of Pharmaceutical Sciences*, *93*(3), 621–634.

Almeida-Prieto, S., Blanco-Méndez, J., & Otero-Espinar, F. J. (2006). Microscopic image analysis techniques for the morphological characterization of pharmaceutical particles: Influence of process variables. *Journal of Pharmaceutical Sciences*, *95*(2), 348–357.

Araszkiewicz, M., Koziola, A., Lupinskaa, A., & Lupinskia, M. (2006). Temperature distribution in a single sphere dried with microwaves and hot air. *Drying Technology*, *24*, 1381–1386.

Arica, B., Çaliş, S., Atİlla, P., Durlu, N. T., Çakar, N., Kaş, H. S., et al. (2005). In vitro and in vivo studies of ibuprofen-loaded biodegradable alginate beads. *Journal of Microencapsulation*, *22*(2), 153–165.

Auriemma, G., Del Gaudio, P., Barba, A. A., d'Amore, M., & Aquino, R. P. (2011). A combined technique based on prilling and microwave assisted treatments for the production of ketoprofen controlled release dosage forms. *International Journal of Pharmaceutics*, *415*(1–2), 196–205.

Bajpai, S. K., & Sharma, S. (2004). Investigation of swelling/degradation behaviour of alginate beads crosslinked with Ca^{2+} and Ba^{2+} ions. *Reactive and Functional Polymers*, *59*(2), 129–140.

Brandenberg, H., & Widmer, F. (1998). A new multinozzle encapsulation/immobilization system to produce uniform beads of alginate. *Journal of Biotechnology*, *63*, 73–80.

Chappard, D., Degasne, I., Huré, G., Legrand, E., Audran, M., & Baslé, M. F. (2003). Image analysis measurements of roughness by texture and fractal analysis correlate with contact profilometry. *Biomaterials*, *24*(8), 1399–1407.

Chiappetta, D. A., Carcaboso, A. M., Bregni, C., Rubio, M., Bramuglia, G., & Sosnik, A. (2009). Indinavir-loaded pH-sensitive microparticles for taste masking: Toward extemporaneous pediatric anti-HIV/AIDS liquid formulations with improved patient compliance. *AAPS PharmSciTech*, *10*(1), 1–6.

Debunne, A., Vervaet, C., Mangelings, D., & Remon, J.-P. (2004). Compaction of enteric-coated pellets: Influence of formulation and process parameters on tablet properties and in vivo evaluation. *European Journal of Pharmaceutical Sciences*, *22*(4), 305–314.

Del Gaudio, P., Colombo, P., Colombo, G., Russo, P., & Sonvico, F. (2005). Mechanisms of formation and disintegration of alginate beads obtained by prilling. *International Journal of Pharmaceutics*, *302*, 1–9.

Del Gaudio, P., Russo, P., Rosaria Lauro, M., Colombo, P., & Aquino, R. (2009). Encapsulation of ketoprofen and ketoprofen lysinate by prilling for controlled drug release. *AAPS PharmSciTech*, *10*(4), 1178–1185.

Elzatahry, A. A., Eldin, M. S. M., Soliman, E. A., & Hassan, E. A. (2009). Evaluation of alginate–chitosan bioadhesive beads as a drug delivery system for the controlled release of theophylline. *Journal of Applied Polymer Science*, *111*(5), 2452–2459.

Fortunato de Carvalho Rocha, W., Sabin, G. P., Março, P. H., & Poppi, R. J. (2011). Quantitative analysis of piroxicam polymorphs pharmaceutical mixtures by hyperspectral imaging and chemometrics. *Chemometrics and Intelligent Laboratory Systems*, *106*(2), 198–204.

Gainotti, A., Losi, E., Sonvico, F., Baroni, D., Massimo, G., Colombo, G., et al. (2006). The effect of residual water on antacid properties of sucralfate gel dried by microwaves. *AAPS PharmSciTech*, *7*, E1–E6.

Geckle, J. M., Rescek, D. M., & Whipple, E. B. (1989). Zwitterionic piroxicam in polar solution. *Magnetic Resonance in Chemistry*, *27*(2), 150–154.

Gong, R., Li, C., Zhu, S., Zhang, Y., Du, Y., & Jiang, J. (2011). A novel pH-sensitive hydrogel based on dual crosslinked alginate/N-[alpha]-glutaric acid chitosan for oral delivery of protein. *Carbohydrate Polymers*, *85*(4), 869–874.

Hegedus, Á., & Pintye-Hódi, K. (2007). Comparison of the effects of different drying techniques on properties of granules and tablets made on a production scale. *International Journal of Pharmaceutics*, *330*(1–2), 99–104.

Jamuna-Thevi, K., Zakaria, F. A., Othman, R., & Muhamad, S. (2009). Development of macroporous calcium phosphate scaffold processed via microwave rapid drying. *Materials Science and Engineering: Part C*, *29*(5), 1732–1740.

Josef, E., Zilberman, M., & Bianco-Peled, H. (2010). Composite alginate hydrogels: An innovative approach for the controlled release of hydrophobic drugs. *Acta Biomaterialia*, *6*(12), 4642–4649.

Kappe, C. O., & Dallinger, D. (2006). The impact of microwave synthesis on drug discovery. *Nature Reviews Drug Discovery*, *5*(1), 51–63.

Kowalczuk, P. B., Sahbaz, O., & Drzymala, J. (2011). Maximum size of floating particles in different flotation cells. *Minerals Engineering*, *24*(8), 766–771.

Li, X., Shen, Q., Su, Y., Tian, F., Zhao, Y., & Wang, D. (2009). Structure–function relationship of calcium alginate hydrogels: A novel crystal-forming engineering. *Crystal Growth & Design*, *9*(8), 3470–3476.

Lidström, P., Tierney, J., Wathey, B., & Westman, J. (2001). Microwave assisted organic synthesis—A review. *Tetrahedron*, *57*(45), 9225–9283.

Loh, Z. H., Liew, C. V., Lee, C. C., & Heng, P. W. S. (2008). Microwave-assisted drying of pharmaceutical granules and its impact on drug stability. *International Journal of Pharmaceutics*, *359*(1–2), 53–62.

McMinn, W. A. M., McLoughlin, C. M., & Magee, T. R. A. (2005). Microwave-convective drying characteristics of pharmaceutical powders. *Powder Technology*, *153*(1), 23–33.

Moneghini, M., Zingone, G., & De Zordi, N. (2009). Influence of the microwave technology on the physical–chemical properties of solid dispersion with Nimesulide. *Powder Technology*, *195*(3), 259–263.

Obeidat, W. M., & Price, J. C. (2006). Preparation and evaluation of Eudragit S 100 microspheres as pH-sensitive release preparations for piroxicam and theophylline using the emulsion-solvent evaporation method. *Journal of Microencapsulation*, *23*(2), 195–202.

Patil, S. B., & Sawant, K. K. (2009). Development, optimization and in vitro evaluation of alginate mucoadhesive microspheres of carvedilol for nasal delivery. *Journal of Microencapsulation*, *26*(5), 432–443.

Sakai, T., Sadataka, M., Saito, M., & Matsushita, K. (1985). Studies of disintregation of liquid column between prodiction of uniform size droplets by vibration method. *ICLASS-85*, *7B*, 2–15.

Soong, D., & Shen, M. (1981). Kinetic network model for nonlinear viscoeleatic properties of entangled monodisperse polymers. I. Steady state flow. *Journal of Rheology*, *25*, 259–273.

Streubel, A., Siepmann, J., & Bodmeier, R. (2002). Floating microparticles based on low density foam powder. *International Journal of Pharmaceutics*, *241*(2), 279–292.

Tam, S. K., Dusseault, J., Polizu, S., Ménard, M., Hallé, J.-P., & Yahia, L. H. (2005). Physicochemical model of alginate–poly-l-lysine microcapsules defined at the micrometric/nanometric scale using ATR-FTIR, XPS, and ToF-SIMS. *Biomaterials*, *26*(34), 6950–6961.

Tostões, R. M., Leite, S. B., Miranda, J. P., Sousa, M., Wang, D. I. C., Carrondo, M. J. T., et al. (2011). Perfusion of 3D encapsulated hepatocytes—A synergistic effect enhancing long-term functionality in bioreactors. *Biotechnology and Bioengineering*, *108*(1), 41–49.

Vrecer, F., Vrbinc, M., & Meden, A. (2003). Characterization of piroxicam crystal modifications. *International Journal of Pharmaceutics*, *256*(1–2), 3–15.

Wong, T. W., Chan, L. W., Kho, S. B., & Sia Heng, P. W. (2002). Design of controlled-release solid dosage forms of alginate and chitosan using microwave. *Journal of Controlled Release*, *84*(3), 99–114.